19.4

EVALUATION OF THE QUIC WIND AND DISPERSION MODELS USING THE JOINT URBAN 2003 FIELD EXPERIMENT DATASET

Michael J. Brown[1], Akshay Gowardhan[1], Matt Nelson[1], Mike Williams[1] and Eric R. Pardyjak[2]

[1]Los Alamos National Laboratory, Los Alamos, New Mexico
[2]University of Utah, Salt Lake City, Utah

1. INTRODUCTION

The Quick Urban & Industrial Complex (QUIC) Dispersion Modeling System has been developed to rapidly compute the transport and dispersion of toxic agent releases in the vicinity of buildings. It is composed of an empirical-diagnostic wind solver, an "urbanized" Lagrangian random-walk model, and a graphical user interface. In this paper, we discuss improvements made to the original Röckle schemes in order to better capture flow fields in dense built-up areas. The model-computed wind and concentration fields are then compared to measurements from the Oklahoma City Joint Urban 2003 field experiment.

2. OVERVIEW OF QUIC

QUIC produces high-resolution 3-D mean wind and concentration fields around buildings, in addition to deposition on the ground and building surfaces. It has options for different release types, including point, moving point, line, area, and volumetric sources, as well as dense gas, explosive buoyant rise, multi-particle size, bio-slurry, and two-phase releases. Other features include indoor infiltration, a pressure solver, outer grid simulations, vegetative canopies, and population exposure calculations. It has been used for biological agent sensor siting in cities, vulnerability assessments for heavier-than-air chemical releases at industrial facilities, and clean-up assessments for radiological dispersal device (RDD) releases in cities (e.g., see Linger et al., 2005; Brown, 2006a, b). QUIC has also been used for dust transport studies (Bowker et al., 2007a) and for the impact of highway sound barriers on the transport and dispersion of vehicle emissions (Bowker et al., 2007b).

a) Wind Solver

The QUIC wind solver is an empirically-based diagnostic wind model based on the ideas of Röckle (1990). The wind solver generates a mass consistent mean wind field around buildings by using various empirical relationships based on the building height, width, and length, and the spacing between buildings to initialize the velocity fields in the regions around buildings (e.g., upwind rotor, downwind cavity and wake, street canyon vortex, and rooftop vortex). This initial flow field is then forced to satisfy mass conservation. For the 2 million grid cell downtown Oklahoma City simulation performed for this evaluation study, the wind field was generated in approximately one minute on a single processor PC. More information about the wind solver can be found in Pardyjak and Brown (2003), Singh et al. (2008), and Gowardhan et al. (2009).

b) Dispersion Model

The QUIC dispersion model is a Lagrangian random-walk code which tracks the movement of gases and aerosols as they disperse through the air. It uses the mean wind field computed by the wind solver and produces the turbulent dispersion of the airborne contaminant using random-walk equations with additional drift terms appropriate for the inhomogeneous nature of turbulence around buildings (Williams et al., 2002). The normal and shear stresses and turbulent dissipation are determined based on similarity theory, gradient transport and a non-local mixing formulation that approximates the turbulent mixing that occurs in building cavities and street canyons. Details regarding the model can be found in Williams et al. (2004).

3. FIELD EXPERIMENT DESCRIPTION

The Joint URBAN 2003 field experiment was held in Oklahoma City in July 2003 and had the goal of obtaining measurements useful for the testing and evaluation of the next generation of urban transport and dispersion models. The experiment consisted of a large number of tracer releases at three different locations in the central business district (CBD) and a network of concentration samplers and in-situ and remote sensing meteorological instrumentation placed in and around the city (Allwine et al., 2004).

During the experiment ten intensive operating periods (IOP's) were conducted over a roughly eight hour period. Three 30-minute point-source releases of sulfur hexafluoride (SF6) at 2 m agl were typically performed during each IOP. Concentration measurements were taken over a one hour period, beginning at the release start

* *Corresponding author address:* Michael Brown, Los Alamos National Laboratory, Los Alamos, NM 87545, e-mail: mbrown@lanl.gov

time and extending thirty minutes beyond the release end time (Clawson et al, 2005).

Bag samplers were placed throughout the downtown area at roughly 3 m above street level and at 1m above roof level. Sampling durations ranged from 5 minutes to 30 minutes. For this study, the concentration measurements were averaged to 30 minutes for comparison to model output.

IOP-2, Release 1 (10:00-11:00 CST, July 2) and IOP-8, Release 2 (00:00-01:00 CST, July 25) were chosen for this evaluation study in order to look at both a daytime and nighttime release within the downtown area. The source location – the so-called "Westin" release – was at the southern edge of the high-rise district just south of Main St. on N. Broadway Ave. a north-south avenue running through the center of the CBD (see Fig. 1).

Prevailing winds were predominately from the south-southwest during IOP-2 and the south-southeast for IOP-8.

4. MODIFICATIONS TO FLOW ALGORITHMS

The original Röckle scheme was developed for low-rise industrial facilities and was shown to perform fairly well for isolated and relatively simple multi-building layouts (Röckle and Richter, 1998; Leitl et al., 1997). In prior efforts, our team has made improvements to the schemes for isolated buildings, including modification of the upwind rotor algorithm (Bagal et al., 2003), the addition of a rooftop recirculation scheme (Pol et al., 2006), and alterations to the cavity length scheme necessary for wide buildings and the upwind rotor algorithm for high-rise buildings (Nelson et al., 2008). Additional building types have also been added, including cylinders, parking garages, and stadia (Nelson et al., 2008).

For dense urban areas, we found that numerous modifications and additional logic were necessary in order to handle the complexity of buildings in these regions. In this section, we qualitatively describe some of the major enhancements we have made to the QUIC wind solver to address the scenarios that result in cities.

a) Order of Flow Algorithm Implementation

One of the main issues when applying the Röckle method to multi-building problems is how to deal with overlapping recirculation zones created by nearby buildings. In the real world, there is likely an interaction of the flow from the overlapping recirculation zones with each altering the other in some fluid dynamical way governed by the Navier-Stokes equations. To implement the Röckle approach, one could weight the over-lapped flow zones from different buildings in some way to create a blended region. How to blend the two interacting recirculation zones, however, is not straightforward and likely difficult to do in a robust universal way.

To keep things simple and easy to implement, we have developed logic for the order in which recirculation zones are introduced, and rules for whether the later zones implemented overwrite earlier ones. The first flow algorithm employed in our scheme is the upwind recirculation flow zone and it is applied to all buildings in the domain before moving on to the second step of applying the downwind building wake and cavity zone algorithms to all buildings. The fourth algorithm implemented is the street canyon and the last is the rooftop recirculation. Below, we describe the reasons for the implementation order of the building flow zones and whether or not they overwrite or modify flow zones that have already been written out. Note that the logic was also designed to reduce computation time by eliminating sorting and searching routines.

In general, a recirculation zone exists on the upwind side of a building if it is not sheltered by other buildings (and the prevailing wind is nearly perpendicular to the front face of the building). That is, the rotor develops only if a strong flow impinges on the front face of the building (note that the upwind scheme is only activated if the impinging flow is close to perpendicular relative to the front face of the building). If other buildings are upwind of the building of interest, and if they are close in distance, the downwind cavity or a street canyon circulation will suppress the formation of the upwind rotor. Hence, the upwind scheme is implemented first so that it can be overwritten or modified by the other flow algorithms later.

The downwind wake zone and downwind cavity zone are applied together building by building. The downwind wake zone is implemented first and acts to reduce the magnitude of the background winds and any upwind recirculation zones that it overlaps, however, it is not allowed to overwrite the downwind cavity zones of other buildings. The thought is that the flow in the wake of one building may still have enough momentum to force an upwind recirculation zone to form on the front face of the downwind building and to cause a low pressure region on the back side of the downwind building which would lead to a recirculation zone. That is, the shielding effect of the upwind building is significantly reduced once the spacing of buildings is large enough that the downwind building is feeling the wake flow of the upwind building. This regime is the wake interference regime as described by Oke (1987). In the real world, the size of the

downwind cavity and upwind recirculation zone of the downwind building are likely altered by the presence of the wake from the upwind building; however, we ignore this effect in our building flow algorithms and only account for the reduced flow strength.

The downwind cavity zone is applied next and overwrites all other flow zones that it overlaps (background flow, wake zones, upwind recirculation zones, and any downwind cavity zones from other buildings already implemented). If one building is immediately downwind of another and if the two buildings are close enough together, then the upwind recirculation zone of the downwind building will be overwritten by the downwind cavity of the upwind building. Although purely a result of the order of implementation of the building flow algorithms, this is exactly the consequence desired. From a fluid dynamics perspective, the upwind recirculation zone would not form on the downwind building because of the sheltering effect of the upwind building. The logic of overwriting allows for this to occur. Note that the order in which the cavity algorithms are applied to the buildings is important and described immediately below in Section 4b.

The next algorithm to be implemented is the street canyon scheme. This scheme is only implemented if the buildings are close enough together to be in the skimming flow regime. If the building height-to-building spacing ratio criterion is met, then the street canyon zone overwrites all of the earlier building flow zones that have been implemented. The street canyon is driven by the wind immediately above the canyon and thus the other building flow zones can influence the direction and strength of the vortex. For example, the reverse flow in the cavity of a tall building results in a vortex that rotates counter-clockwise in the street canyon zone between the two buildings. This phenomenon has been documented in computational fluid dynamics modeling (e.g., Hu and Wang, 2005), although it's not clear how persistent such a vortex structure would be in real life.

The last zone to be implemented is the rooftop recirculation zone. By being at the end, the rooftop recirculation zone can be driven by the proper reference velocity (both magnitude and direction), that is, a reference velocity that reflects the effects of the buildings via the flow parameterizations already implemented. The rooftop recirculation zone, however, is not implemented if the rooftop zone is within a downwind cavity zone. The implication is that the reverse flow found in the cavity would not be strong enough to cause separation at the leading edge of the smaller building embedded within the cavity zone. We have found no experimental data or CFD modeling calculations that confirm or contradict this supposition. In addition, we have logic that does not allow a rooftop recirculation to form on the downwind building forming a street canyon since there would be minimal blockage on the front face of the downwind building and thus rooftop separation would likely not occur.

b) Downwind Cavity Zone Small-to-Tall Logic

As indicated earlier, one of the main issues when applying the Röckle method to multi-building problems is how to deal with overlapping building flow regions from different buildings in the vicinity of one another. Since we have implemented logic that results in flow zones being overwritten, there is an issue with which building to begin with and so forth, especially when implementing the downwind cavity zones. For example, if the downwind cavity zone of a taller building is predicted to overlap with a smaller downwind building, how does one initialize the flow field in this overlapped region? We have devised a so-called "small-to-tall" logic, where building flow algorithms are implemented in building-height order beginning with the smallest building. For example, in a two building case where the upwind building is larger, the downwind cavity is first created for the smaller building. The cavity zone for the taller building is then specified. If the cavity zone of this tall building overlaps the smaller building, we allow the tall building cavity zone to overwrite the smaller building flow zones (based on the flow algorithm order of implementation that includes the upwind recirculation zone and the downwind cavity zone). This logic was devised because the taller upwind building shields the smaller downwind building, and thus the reason for the development of the upwind rotor and the downwind cavity zone (strong winds impacting the front face of the building, flow separation at the leading edge of the roof of the building, and the low pressure zone on the backside of the building) would not exist. Note that if the upwind building is narrower in cross-wind dimension, then only part of the upwind rotor and cavity zone of the wider, but shorter downwind building will be overwritten.

c) Stacked Building Logic

To make complex buildings that vary in plan area with height, QUIC allows building shapes to be stacked. This results in the need to modify the downwind cavity and wake, and street canyon algorithms to properly account for the "buildings" stacked on other buildings.

The street canyons are applied using the small-to-tall logic as well. If buildings are stacked, the street canyon zones implemented for the base buildings are overwritten later by the street

canyon zones from the taller stacked buildings. The algorithm is modified so that the street canyon zone extends to the ground rather than to just the base of the building.

For downwind cavities, we found that simply overwriting the cavity of the base building by the cavity of the taller stacked building often produced unrealistic flow fields when the stacked building was narrower in the cross-wind direction. In reality, the cavity of the narrower stacked building should not penetrate to the ground, but only some fractional depth below the base of the stacked building. To account for this, we developed a method which reduces the effective base height of the stacked building according to the ratio of the widths of the base and stacked buildings. As the width of the stacked building approaches the width of the base building, the effective base height of the stacked building will approach the ground**.** That is, the cavity of the stacked building drops below its base, but not to the ground, unless the buildings are of equal width.

d) Reduced Cavity Length in Built-up Zones

Based on wind-tunnel data sets and CFD calculations, we found that the cavity downwind of a building is foreshortened if there are buildings downwind of it. Here we are considering a case where the buildings are not close enough together where a street canyon would form (in the intermediate zone of wake interference flow) or smaller buildings are downwind of taller buildings. The shortening of the cavity length makes sense in the latter case because the downwind buildings block the backflow at street level, thus cutting off the circulation in the cavity. For equal height buildings, this effect also becomes apparent in intersections for oblique angle flows.

5. MODEL SET-UP

The QUIC modeling domain covers most all of the Oklahoma City central business district (CBD) and is 1.2 km x 1.2 km in size. The horizontal grid size was set to 5 m, while the vertical resolution was set to 3 m resulting in a 240 by 240 by 60 grid cell domain (3.5 million cells total). Earlier studies with higher horizontal grid resolution indicated that the plume simulations were not sensitive to the grid size and so the simulations were performed using the 5 m grid size. The 3D building data were obtained from the Defense Threat Reduction Agency and the University of Oklahoma. Although there were trees in the downtown area, the simulations performed for this study were done without the vegetation canopy scheme turned on.

There were a number of wind sensors on towers and remote sensing sodars located upwind of the CBD that could be used to create an inflow profile. The closest upwind location was about 200 meters due south (upwind) of our domain. A Dugway Proving Ground (DPG) propeller anemometer was located on a tower 35 m above the ground and 25 m above the roof of a post office building. The anemometer was not operating, however, during IOP 2. Eight sonic anemometers from Indiana University (IU) were located between 2 m and 80 m above ground level on several towers about 5 km south of our domain. For IOP2, only two sonics provided information, however. A sodar from the Pacific Northwest National Laboratory (PNNL) located about 1 km south-southwest of the CBD was used for the winds above 100 m. We found that the Botanical Gardens Argonne National Laboratory (ANL) sodar located in the southwest corner of our domain also provided reasonable inflow information if the winds were from the southwest, but not if they were from the southeast (probably due to larger buildings being directly southeast of the sodar). In addition we used two other ANL sodars that were downwind of the city to cross correlate with the upwind measurements.

The inflow wind speed profile was created by fitting a log-law to the IU sonics, the DPG prop-vane and the PNNL sodar measurements. A good fit was obtained with a roughness length of 0.1 m and a wind speed at 50 m agl of 5 m/s ($u^* = 0.32$ m/s) for IOP-2 and 7 m/s ($u^* = 0.45$ m/s) for IOP-7. The specification of the inflow wind direction profile was somewhat more difficult as the different instrumentation often showed up to 30º differences in wind direction, with little consistent bias between instrument location and time periods. The scatter wasn't always uniform, with one cluster of measurements at one end of the 30º scatter and another cluster at the other end.

To overcome this problem we followed the method proposed by Coirier et al. (2007). Here, a CFD code is run and the inflow wind direction is varied until the CFD code wind output best matches the surface wind measurements. Running the QUIC-CFD code (Gowardhan et al, 2009) at 10º increments within the 30º range of the measurements, we found that an inflow direction of 200º for IOP-2-release-1 and 170º degrees for IOP-8-release-2 best matched the street-level wind measurements. These were then used as the inflow for the QUIC wind solver calculations. Although the fifteen minute averaged measurements indicated some wind direction variation with time and with height, there was little consistency among the sensors across time periods and with height. Hence, we opted to

use a non-time varying wind profile with the wind direction constant with height.

The atmospheric stability for the simulations was assumed to be neutral. Within the urban canopy this assumption is likely valid, but above the canopy there may be a stable layer during IOP8 and an unstable layer during IOP2. Numerous studies have shown that a several hundred meter well-mixed neutrally-stratified layer often exists above larger-sized city centers due to enhanced thermal and mechanical mixing effects. The downtown district of Oklahoma City is rather small, however, and thus it is not clear if the well-mixed layer is deep or shallow.

6. MODEL EVALUATION

QUIC 5.2 and 4.7 were used for this evaluation study. Version 5.2 was run with all of the newest parameterizations turned on, while 4.7 was run with our implementation of the original Röckle parameterizations. In both cases, the QUIC random-walk dispersion model was run with 300,000 marker particles.

a) IOP2, Release 1

Figure 2 shows the thirty-minute averaged measured and computed concentrations in downtown Oklahoma City during the 10:00-10:30 CST release period. The new scheme appears to accurately capture the western boundary of the plume. The measurements show little westward transport along Main St., Park Ave., Kerr Ave. and McGee Ave and the new scheme mimics this sharp drop off in concentrations from Broadway westward. The old scheme shows appreciable concentrations in these streets to the west of Broadway, whereas the measurements show no concentration reached these locations. The extent of the plume to the east cannot be quantified due to lack of measurements.

The new scheme appears to overestimate the upwind transport immediately south of the release point. The old scheme matches the data better here. This latter result, however, is due to a fortuitous shortcoming in the original scheme which allows a street canyon circulation to form in Broadway between the two buildings immediately north of the Convention Center. Concentrations in the northern half of the domain (4 to 6 blocks downwind of the release point) are overestimated in both cases, indicating that the vertical mixing is likely underestimated.

The paired-in-space and time scatterplots of measured versus computed concentrations shown in Fig. 3 reflect the findings noted above. In addition to the one-to-one line, the plots also contain factor of two and factor of five lines. Qualitatively, the old scheme appears to have a slightly larger number of measurements that it has overestimated by a factor of five or more. The old scheme also has more values on the y-axis (the model produced non-zero values, whereas the measurements were zero), indicative of the overestimation of the westward transport of the model-computed plume using the old scheme. In fact, the new scheme matched 37 of the zero measurements, while the old scheme only matched 31. The new scheme has 24% of the model-computed concentrations within a factor of two, while the old scheme has 20% (note: these numbers do not include the matched zeros). The number of computed concentrations within a factor of five jumped from 48% for the old scheme to 60% for the new scheme.

Figure 4 compares the model-computed and measured thirty minute averaged concentrations from 10:30-11:00 CST after the release was turned off. Overall, the new scheme appears to have captured the boundaries of the plume better than the old scheme, as well as the magnitude of the concentrations. Especially near the source there is a tendency for the old scheme to overestimate the concentrations, indicating that the flushing out of the contaminant is too slow. The scatterplots in Fig. 5 reveal much better agreement between the model-predicted and measured concentrations for the new scheme. The new scheme has 40% of the model predictions within a factor of two, while the old scheme only has 24%. For factor of five, the number jumps to 80% for the new scheme as compared to 44% for the old scheme.

b) IOP8, Release 2

Figure 6 shows that both schemes give fairly similar results for the 00:00-00:30 period just after midnight during the release. The thirty minute averaged plume footprints are fairly similar in both cases. The westward extent of the plume is slightly underestimated in both cases. The upwind transport is much smaller, however, for the new scheme and appears to better match data there. In addition, the old scheme overestimates the amount of material transported to the east on Main St, whereas the new scheme agrees better with the measurements. On the other hand, the new scheme appears to keep the concentrations too high far from the source along Broadway as the orange band extends off the domain. We postulate that the lower concentrations found along Broadway for the old scheme are a result of the portion of the plume getting caught in the downwind cavity of the tall Bank One building, just to the northwest of the release point, lofting part of the plume high into the air and thereby reducing ground-level concentrations. We are currently investigating why the new scheme results in different wind patterns in this area.

The scatterplots for the 00:00 to 00:30 time period are fairly similar for the new and old scheme (Fig. 7). There are a large number of data points on the x-axis, signifying that the model computes zeros for many locations whereas the measurements are recording small non-zero values. In addition, both cases show significant overestimation of mid-range concentrations, demonstrating that for this release the model is not diluting the ground-level concentrations fast enough. The number of model-computed concentrations is slightly better for the new scheme: 23% compared to 16%. The factor-of-five percentages are better for the new scheme as well: 53 to 42%.

The thirty minute averaged concentrations between 00:30-01:00 CST after the release was turned off are shown in Fig. 8. The plume footprint and concentration levels appear fairly similar for the two schemes. The scatterplots in Fig. 8 indicate better agreement between the model-predicted and measured concentrations for the new scheme. The new scheme has 29% of the model predictions within a factor of two, while the old scheme only has 14%. The new scheme has 64% of the computed values within a factor of five, while the old scheme has only 46%.

In summary, for the two releases studied here, It is clear that the new scheme has resulted in higher FAC2 and FAC5 scores as compared to the old scheme. In addition, model performance was generally better for IOP2, Release 1 and that for both IOP's the percentages were higher for the second thirty minute period after the release was turned off (the flushing phase) as compared to the first thirty minute period when the release was still on.

7. CONCLUSION

The QUIC dispersion modeling system was evaluated against two releases from the Oklahoma City Joint Urban 2003 field experiment. The QUIC wind model is based on the Rockle (1990) methodology and has been modified to work better in dense complex cities. The new algorithms were shown to result in better plume concentration predictions as compared to an earlier version of the QUIC code.

6. REFERENCES

Allwine, K.J., M. J. Leach, L. W. Stockham, J. S. Shinn, R. P. Hosker, J. F. Bowers, J. C. Pace, 2004: Overview of Joint Urban 2003 An Atmospheric Dispersion Study in Oklahoma City, AMS Symposium on Planning, Nowcasting, and Forecasting in the Urban Zone, 11-15 January, Seattle, WA.

Bagal, N., E. Pardyjak, and M. Brown, 2003: Improved upwind cavity parameterization for a fast response urban wind model, AMS Conf. on Urban Zone, Seattle, WA, 3 pp.

Bowker, G., R. Baldauf, V. Isakov, A. Khlystov, and W. Petersen, 2007b: The effects of roadside structures on the transport and dispersion of ultrafine particles from highways, At. Env. 41, 8128-8139.

Bowker, G., D. Gillette, G. Bergametti, B. Marticorena, and D. Heist, 2007a: Sand flux simulations at a small scale over a heterogeneous mesquite area of the northern Chihuahuan desert, J. Appl. Meteor., 46, 1410-1422.

Brown, 2007a: Radiological dispersal device (RDD) modeling in cities using the QUIC model, poster, 2007 Fall AGU Meeting, San Francisco, CA. LA-UR-07-3182, http://www.lanl.gov/projects/quic.

Brown, 2007b: Chemical dense gas modeling around buildings using the QUIC model, poster, Fall AGU Meeting, San Francisco, CA, LA-UR-07-3182, http://www.lanl.gov/projects/quic.

Clawson, K., and co-authors, 2005: Joint Urban 2003 (JU03) SF6 atmospheric tracer field tests, NOAA Tech. Memo. OAR ARL-254, 379 pp.

Coirier, W.J., S. Kim, S.C. Ericson, and S. Marella, 2007: Calibration and use of site-specific urban weather observations data using microscale modeling, 87th Annual AMS, Symp. on Met. Obs. & Instru., paper 5.4, 11 pp.

Gowardhan, A., M. Brown, E.R. Pardyjak, 2009: Evaluation of the QUIC Pressure Solver for using wind-tunnel data from single and multi-building experiments, J. Env. Fluid Mech., submitted.

Gowardhan, A., Pardyjak, E.R., Senocak I. and Brown, M.J., 2007: A CFD-based wind solver for a fast response dispersion model, to be submitted to Atmos. Env.

Gowardhan, A., M. Brown, M. Williams, E. Pardyjak, 2006: Evaluation of the QUIC Urban Dispersion Model using the Salt Lake City URBAN 2000 Tracer Experiment Data - IOP 10. 6th AMS Symp. Urban Env., Atlanta, GA, LA-UR-05-9017, 13 pp.

Hu C.-H. and F. Wang, 2005: Using a CFD approach for the study of street-level winds in a built-up area, Building & Environ., v 40, 617-631.

Leitl, B., P. Kastner-Klein, M. Rau, R. Meroney, 1997: Concentration and flow distributions in the vicinity of U-shaped buildings: wind-tunnel and computational data, J. Wind Eng. & Ind. Aerodyn., v 67-68, pp 745-755.

Linger, S., M. Brown, W.B. Daniel, A. Ivey, T. McPherson, M. Williams, and K. Omberg, 2005: Sensing threats with BioWatch, GeoIntelligence, Mar/Apr 2005, pp. 16-21, LA-UR-05-0799.

Nelson, M., B. Addepalli, F. Hornsby, A. Gowardhan, E. Pardyjak, and M. Brown: Improvements to fast-response urban wind model, 15th AMS/AWMA Met. Aspects Air Poll., LA-UR-08-0206, 6 pp.

Oke, T., 1987, Boundary Layer Climates, Routledge, London

Pardyjak, E. and M. Brown, 2001: Evaluation of a fast-response urban wind model – comparison to single-building wind-tunnel data, Int. Soc. Environ. Hydraulics, Tempe, AZ, LA-UR-01-4028, 6 pp.

Pardyjak, E.R. and M. Brown, 2003: QUIC-URB v. 1.1: Theory and User's Guide, LA-UR-07-3181, 22 pp.

Pol S., N. Bagal, B. Singh, M. Brown, and E. Pardyjak, 2006: Implementation of a rooftop recirculation parameterization into the QUIC fast response wind model, 6th AMS Urb. Env. Symp., Atlanta, GA, LA-UR-05-8631, 19 pp.

Röckle, R., 1990: Bestimmung der stomungsverhaltnisse im Bereich Komplexer Bebauugsstrukturen. Ph.D. thesis, Vom Fachbereich Mechanik, der Technischen Hochschule Darmstadt, Germany.

Röckle, R. and C.-J. Richter, 1998: Ausbreitung von Emissionen in komplexer Bebauung – Vergleich zwischen numerischen Modellen und Windkanalmessungen, Förderkennzeichen: PEF 295002, 92 pp.

Singh, B., B. Hansen, M. Brown, E. Pardyjak, 2008: Evaluation of the QUIC-URB fast response urban wind model for a cubical building array and wide building street canyon, *Env. Fluid Mech.,* v 8, pp 281-312.

Williams, M. D., M. J. Brown, and E. R. Pardyjak, 2002: Development of a dispersion model for flow around buildings, 4th AMS Symp. Urban Env., Norfolk, VA, May 20-24 2002, LA-UR-02-0839.

Williams, M., M. Brown, B. Singh, & D. Boswell, 2004: QUIC-PLUME Theory Guide, LA-UR-04-0561, 22 pp.

Figure 1. A Google Earth map of downtown Oklahoma City, roughly the size of our computational domain. The yellow star shows the approximate location of the “Westin” release.

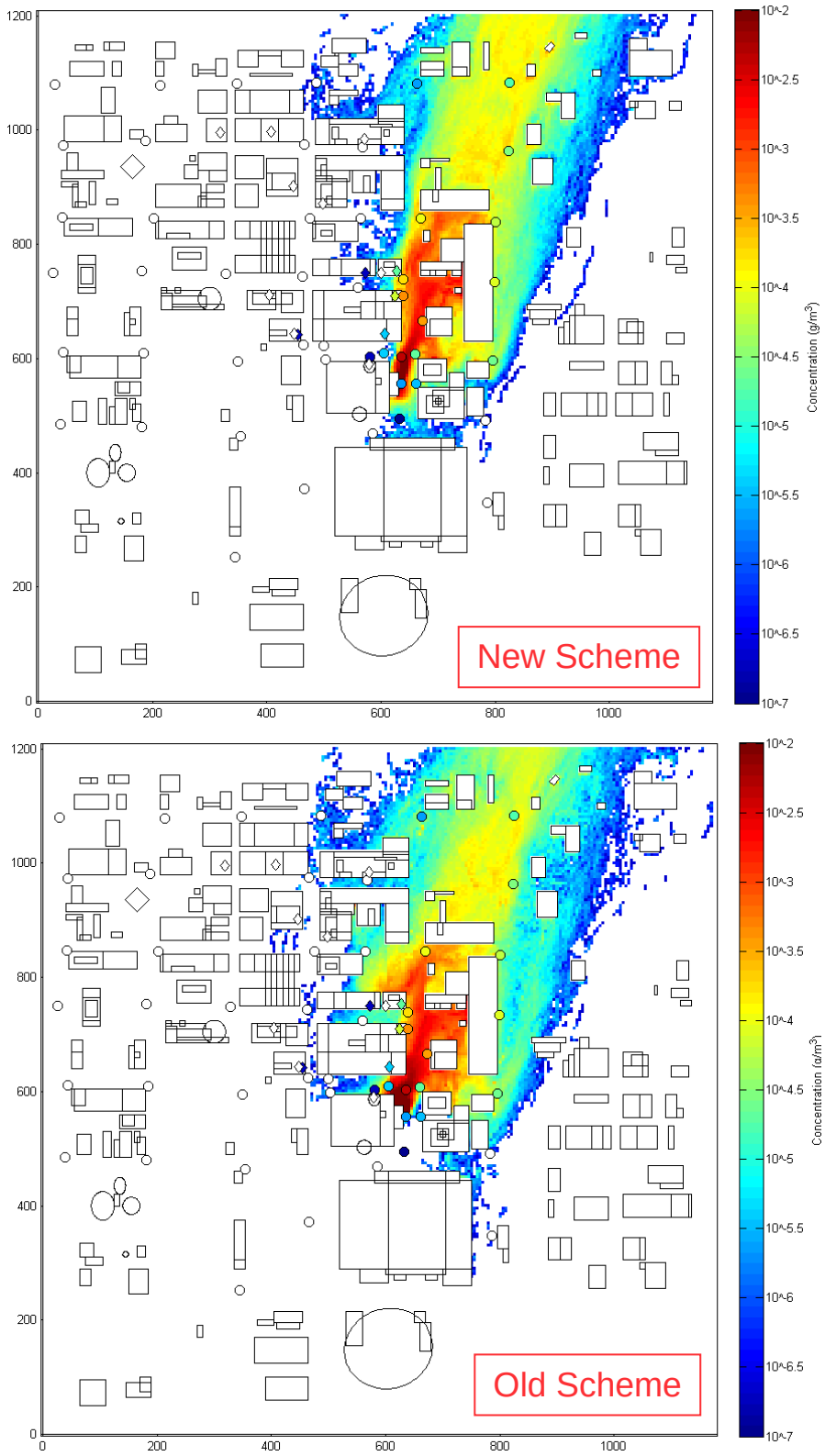

Figure 2. IOP2, Release 2, 10:00-10:30 CST, July 2, 2003 (Release On). Comparison of thirty minute average concentrations measurements at 3 m agl (filled circles) to QUIC using (top) new scheme and (bottom) old scheme. Note: rooftop measurements denoted by triangles.

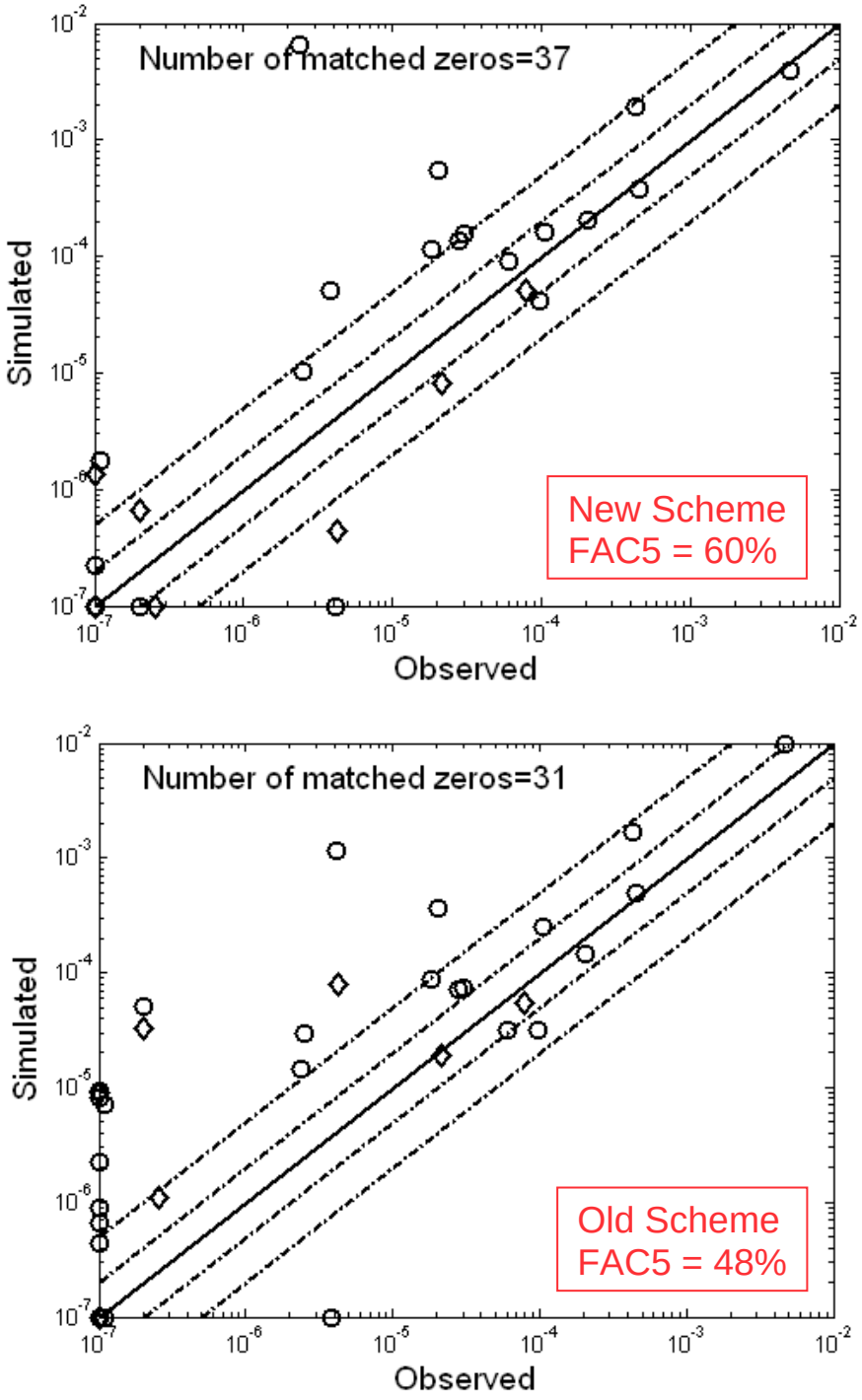

Figure 3. IOP2, Release 2, 10:00-10:30 CST, July 2, 2003 (Release On). Paired-in-space and time scatterplots of QUIC model-computed and measured thirty minute average concentrations: top - new scheme; bottom - old scheme. Circles are near-ground measurements, triangles are rooftop measurements. Factor-of-two and factor-of-five lines shown.

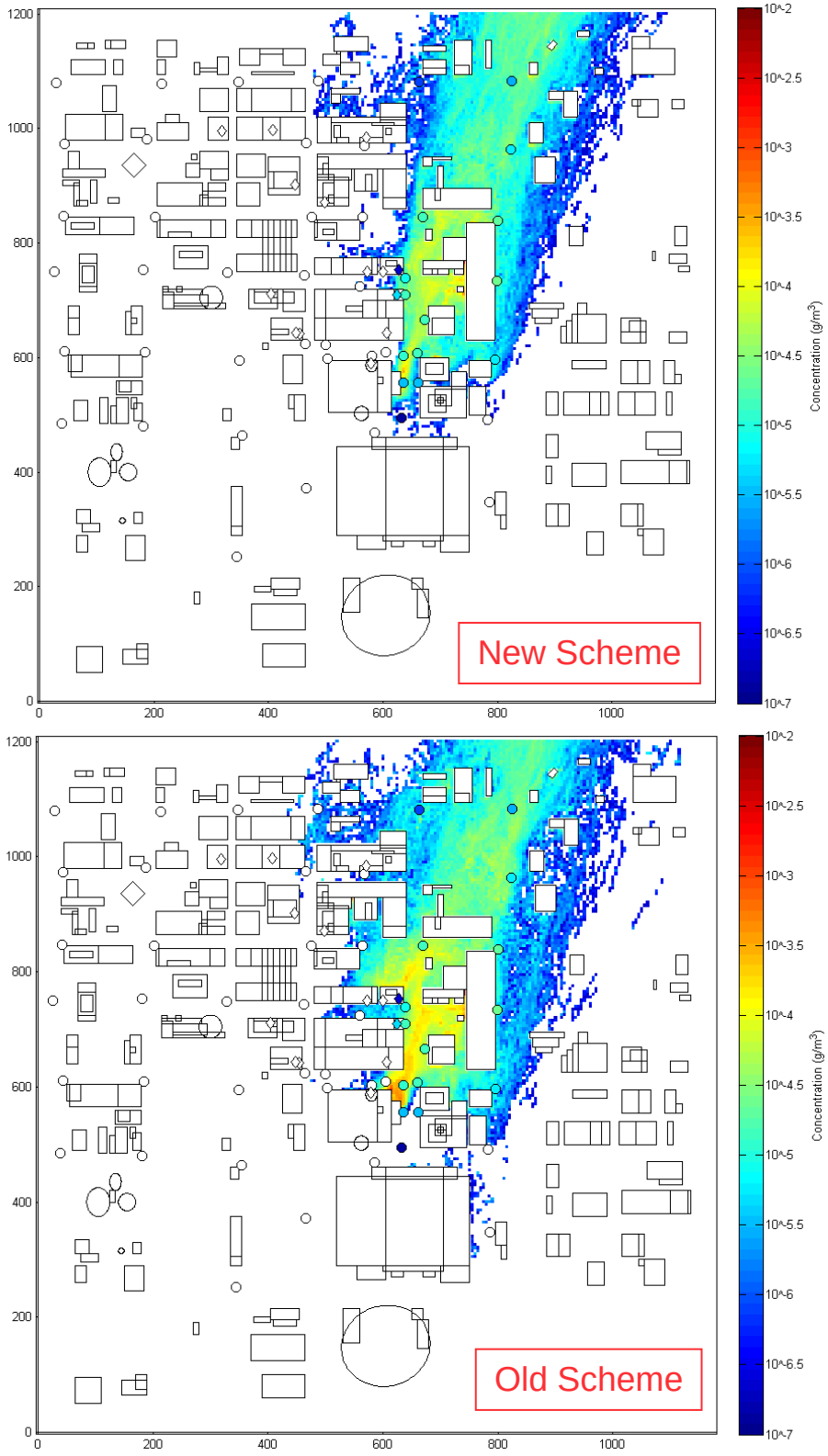

Figure 4. IOP2, Release 2, 10:30-11:00 CST, July 2, 2003 (Release Off). Comparison of thirty minute average concentrations measurements at 3 m agl (filled circles) to QUIC using (top) new scheme and (bottom) old scheme. Note: rooftop measurements denoted by triangles.

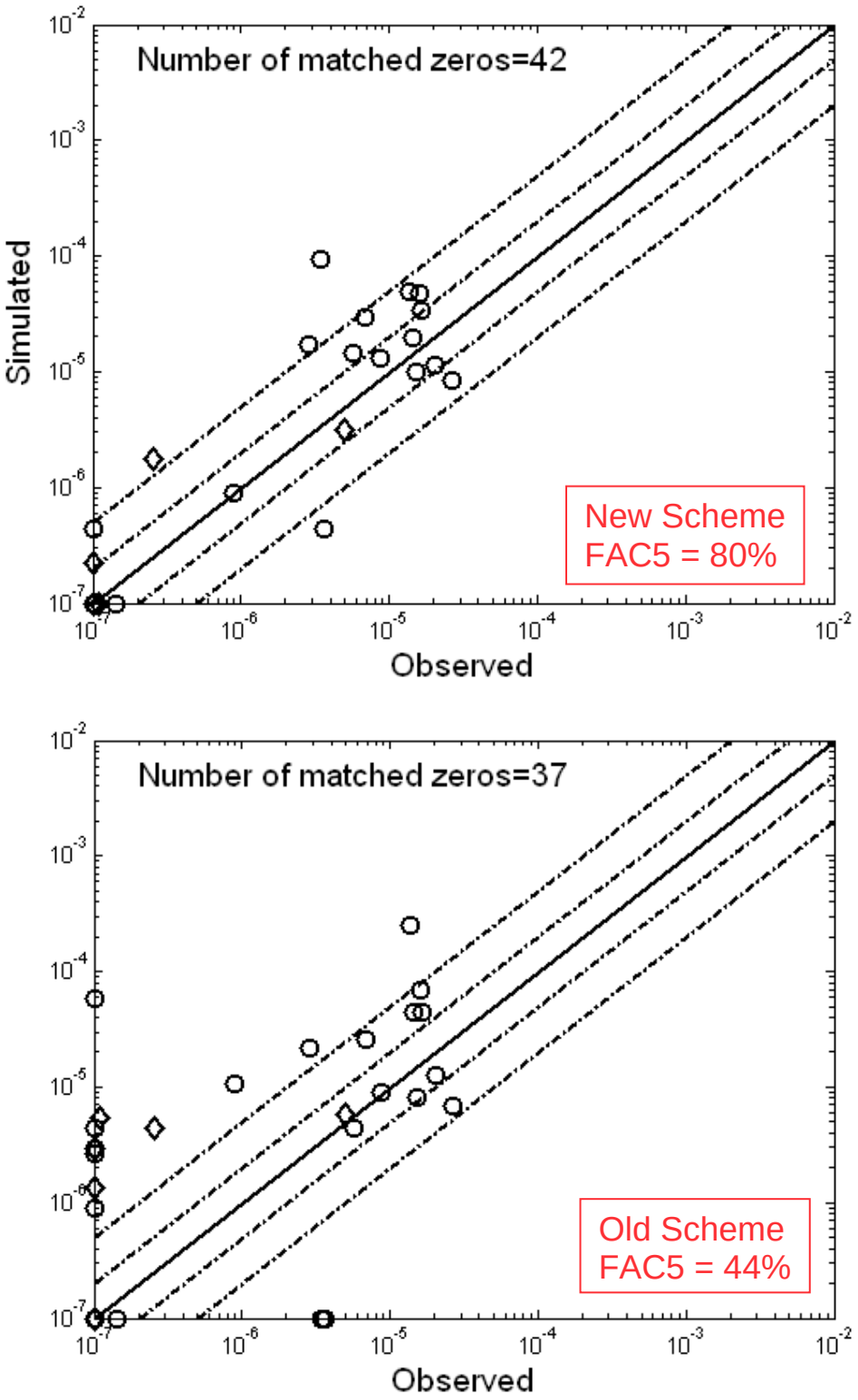

Figure 5. IOP2, Release 2, 10:30-11:00 CST, July 2, 2003 (Release Off). Paired-in-space and time scatterplots of QUIC model-computed and measured thirty minute average concentrations: top - new scheme; bottom - old scheme. Circles are near-ground measurements, triangles are rooftop measurements. Factor-of-two and factor-of-five lines shown.

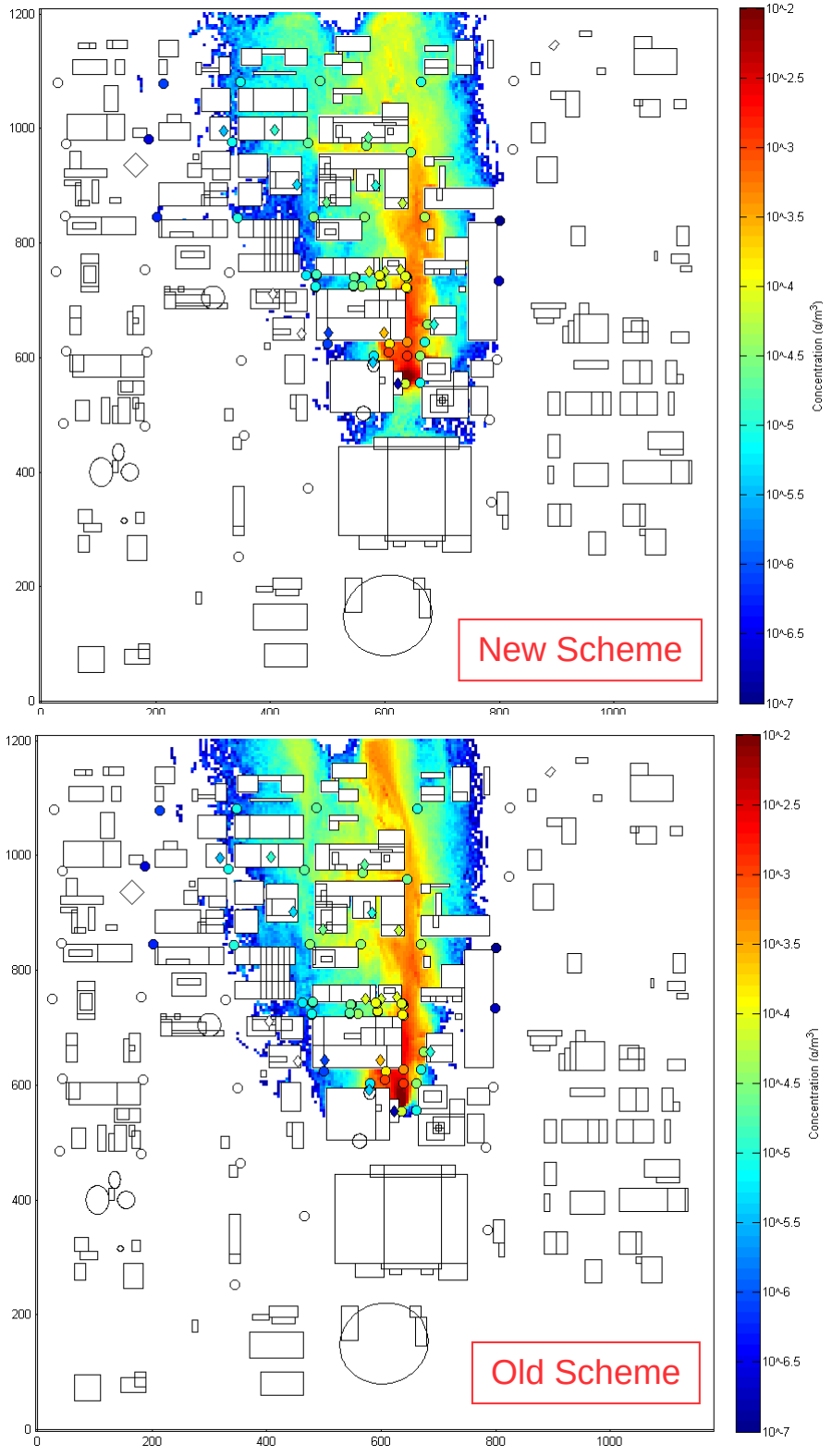

Figure 6. IOP8, Release 1, 00:00-00:30 CST, July 25, 2003 (Release On). Comparison of thirty minute average concentrations measurements at 3 m agl (filled circles) to QUIC using (top) new scheme and (bottom) old scheme. Note: rooftop measurements denoted by triangles.

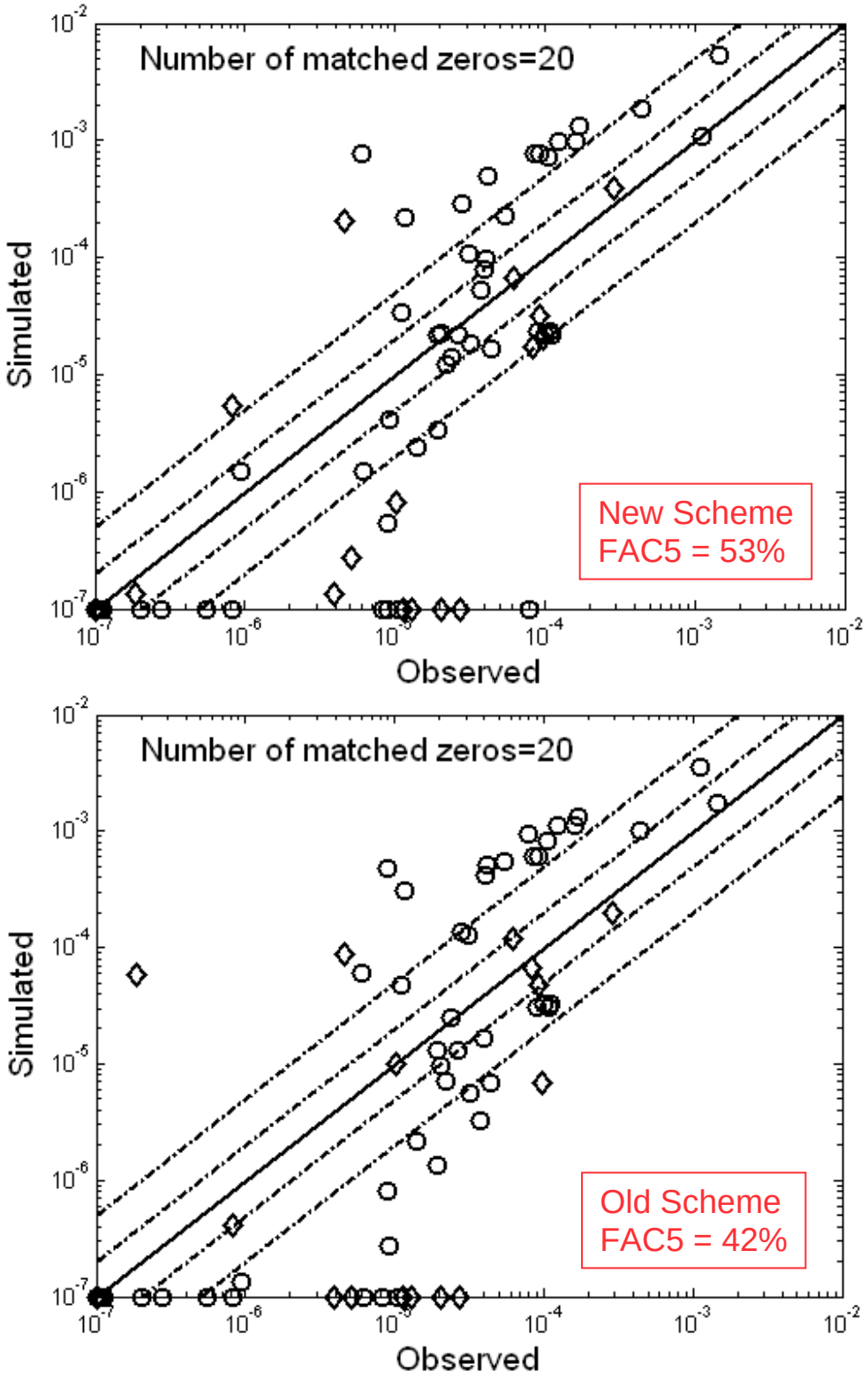

Figure 7. IOP8, Release 1, 00:00-00:30 CST, July 25, 2003 (Release On). Paired-in-space and time scatterplots of QUIC model-computed and measured thirty minute average concentrations: top - new scheme; bottom - old scheme. Circles are near-ground measurements, triangles are rooftop measurements. Factor-of-two and factor-of-five lines shown.

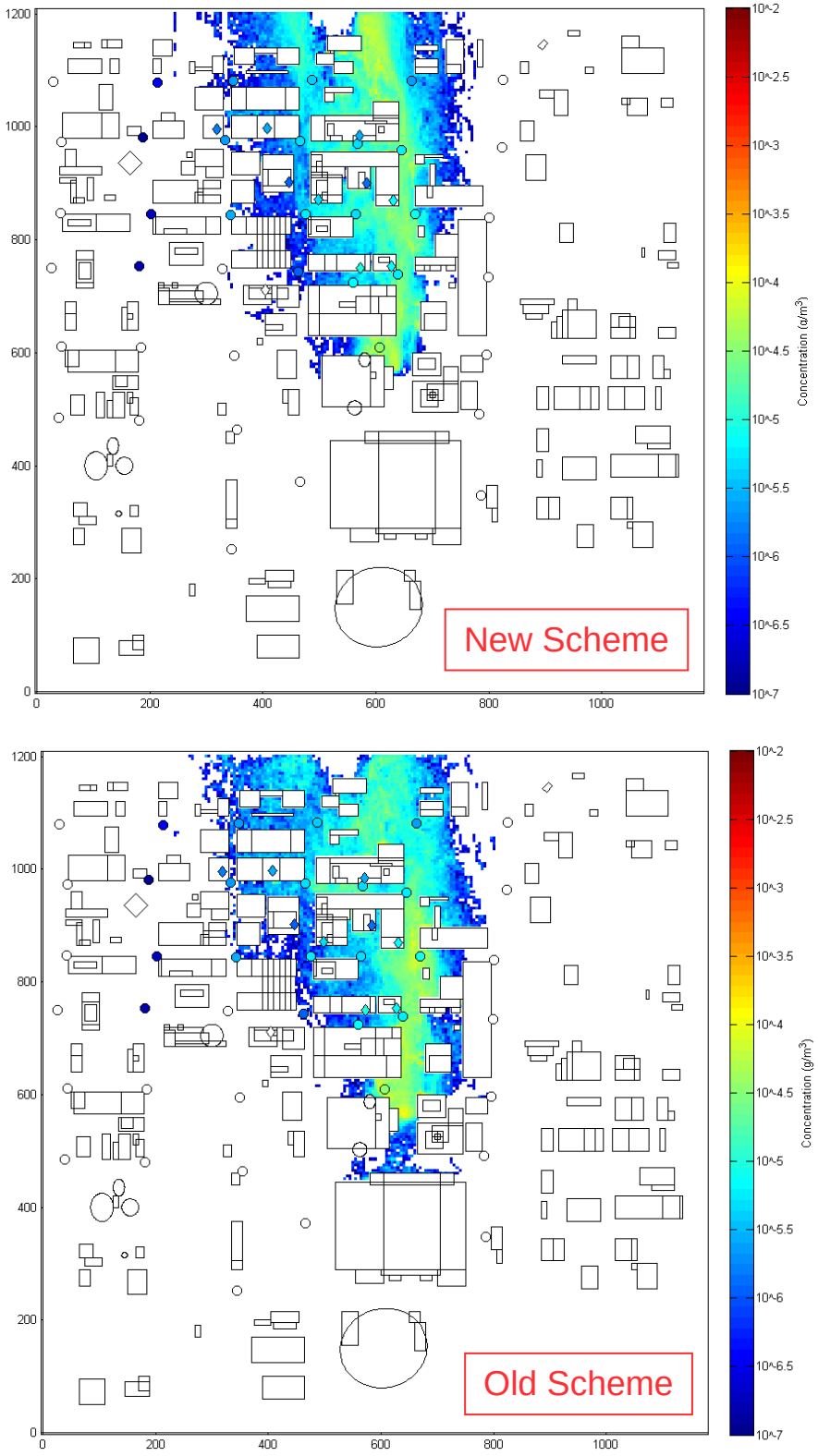

Figure 8. IOP8, Release 1, 00:30-01:00 CST, July 25, 2003 (Release Off). Comparison of thirty minute average concentrations measurements at 3 m agl (filled circles) to QUIC using (top) new scheme and (bottom) old scheme. Note: rooftop measurements denoted by triangles.

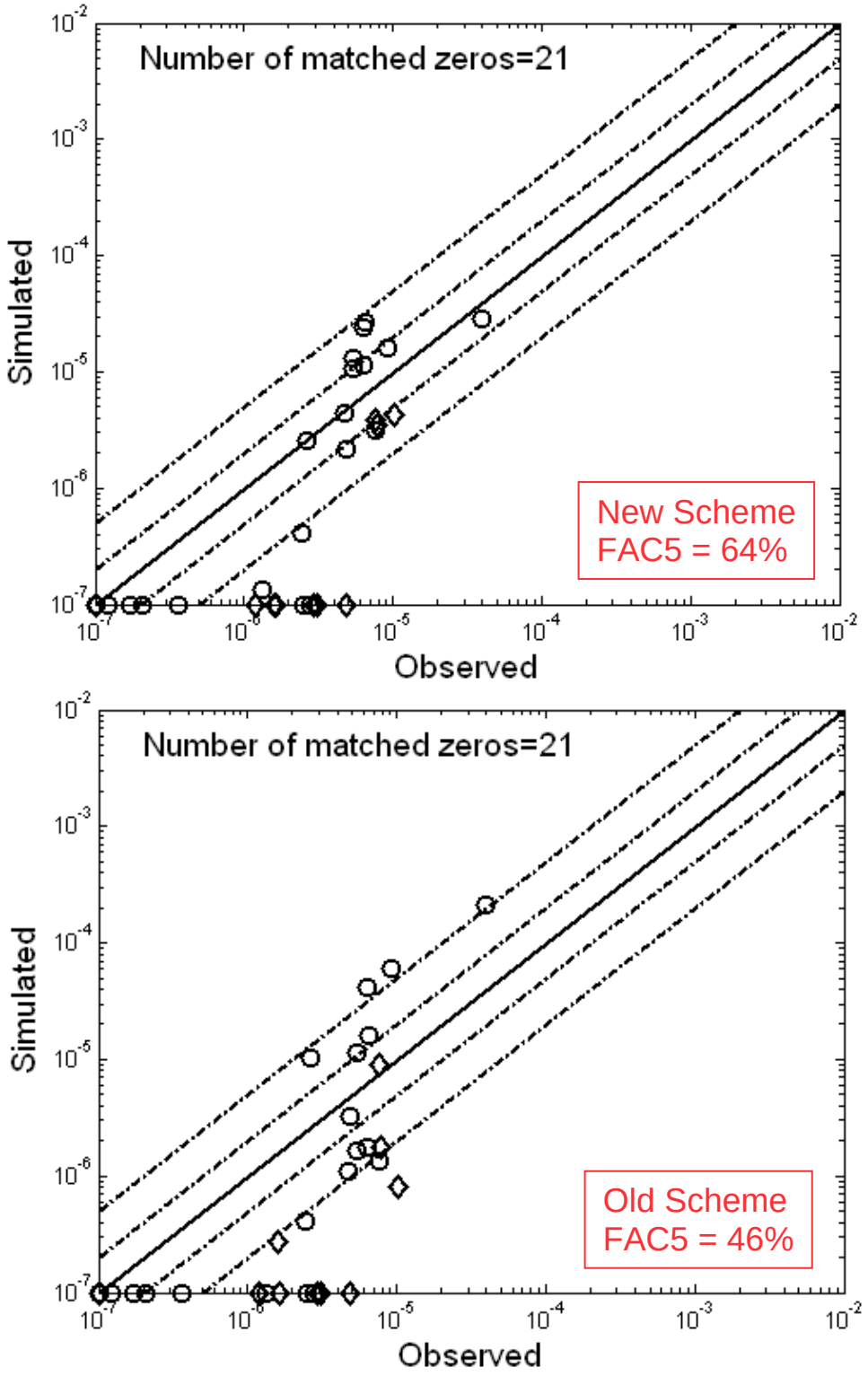

Figure 9. IOP8, Release 1, 00:30-01:00 CST, July 25, 2003 (Release Off). Paired-in-space and time scatterplots of QUIC model-computed and measured thirty minute average concentrations: top - new scheme; bottom - old scheme. Circles are near-ground measurements, triangles are rooftop measurements. Factor-of-two and factor-of-five lines shown.